Protection of cobalt-based refractory alloys by chromium deposition on surface. Part I: Sub-surface enrichment in chromium by packcementation and diffusion

Grégory Michel, Patrice Berthod, Michel Vilasi, Stéphane Mathieu, Pierre Steinmetz

Protection of cobalt-based refractory alloys by chromium deposition on surface. Part I: Sub-surface enrichment in chromium by pack-cementation and diffusion

Grégory Michel, Patrice Berthod*, Michel Vilasi, Stéphane Mathieu, Pierre Steinmetz

Institut Jean Lamour, Department Chemistry and Physics of Solids and Surfaces, Team 206,
Faculty of Sciences and Technologies, University Henri Poincaré Nancy 1,
B.P. 70239, 54506 Vandoeuvre-lès-Nancy, France

Post print of the article *Surface & Coatings Technology 205 (2011) 3708–3715*
doi:10.1016/j.surfcoat.2011.01.027

Abstract

The feasibility of surface chromium enrichment by pack-cementation was assessed for different low chromium-containing cobalt alloys, in order to improve their resistance against high temperature. A binary Co-10Cr alloy, two ternary Co-10Cr-0.5C and Co-10Cr-1.0C alloys and two TaC-containing Co-10Cr-based alloys were elaborated by foundry for the study. 7.5h-long and 15h-long cementations at 1050°C, followed or not by a 75h-long heat treatment at 1200°C were performed on these alloys. Microstructure examinations performed using a Scanning Electron Microscope and concentration profiles using Electron Probe Micro Analysis – Wavelength Dispersion Spectrometry were realized in order to analyze the level of Cr-enrichment of the sub-surface region, with as studied criteria: the nature of the external Cr-enriched zone, the maximal chromium content on surface and the depth of chromium enrichment. The Cr-enrichment of the sub-surface succeeded for the Co-10Cr alloy and for the two tantalum-containing alloys, with the formation of an external metallic zone containing around 30wt.%Cr. In contrast the chromium carbides – containing alloys were effectively enriched in chromium in surface but in the form of a continuous chromium carbide layer which can induce other problems such as spallation and then possible fast oxidation of the denuded alloy. Finally it appeared that only the carbon-free alloys, and the alloys reinforced by carbides more stable than chromium carbides, are potentially able to be successful enriched in chromium in their sub-surface by pack-cementation.

Keywords: Cobalt-based alloys; Pack-cementation; Chromium; Carbides

*Corresponding author: Patrice Berthod
Tel.: +33 3 83 68 46 66
Fax.: +33 3 83 68 46 11
E-mail: patrice.berthod@centraliens-lille.org

1. Introduction

Turbine blades located behind the combustion chamber in jet engines, as well as the metallic pieces working in the high temperature zones of some industrial machines, are exposed to hot oxidant gases, and in some cases also to aggressive liquid substances as molten salts. This induces a surface deterioration which is one of the reasons limiting the lifetime of these pieces [1]. These phenomena can be slowed down by the addition, to the chemical composition of the alloys, of sufficient amounts of elements allowing the formation of protective oxide scales separating the bulk from oxidant gases [2]. These elements can be chromium (e.g. in cobalt-based alloys [3]), aluminum (e.g. in nickel-based superalloys [4]) or silicon (e.g. in other alloys, based on molybdenum or niobium [5]). In the case of alloys containing a sufficient amount of chromium, selective oxidation leads – after a short time – to the formation of an external continuous chromia (Cr_2O_3) layer which protects the alloys from further rapid oxidation. In order to guarantee such a chromia-forming behavior in the case of cobalt-based superalloys it is usually considered that this amount must be about 30wt.% Cr. However, such high chromium content may significantly lower the solidus temperature of the alloy, and then – potentially – its creep resistance. In addition to chromium, cobalt-based superalloys contain high amounts of strengthening elements, present in solid solution, such as tungsten or molybdenum. Such elements favor with chromium the precipitation of brittle phases, during either the elaboration process (solidification and heat-treament) or in service. Hence it appears preferable for these alloys to have limited chromium content to ensure high mechanical performances at elevated temperature, and a sub-surface especially chromium-rich to resist to hot corrosion. This surface enrichment in Cr can be obtained by chromium deposition using the pack-cementation technique.

Pack-cementation is a well-known method allowing depositing one or more elements on the surface of a metallic piece. This technique has been employed for several tens of years to enrich the surface of various substrates with elements which can be of different natures: for example Al on niobium alloys [6], nickel-based alloys [7,8] or cobalt alloys [9], Si on steels [10] and nickel alloys [11], B on iron- [12] and titanium-based [13] alloys, and even Mn on steels [14]. Works concerning the protection of alloys by deposits obtained by pack-cementation continue to be carried out today as illustrated by the following several research articles choosen among the most recent ones: aluminum on steels [15], on nickel-based alloys [16] and on Mo-Si-B alloys [17], silicon on niobium-based alloys [18,19] and on molybdenum and/or tungsten-based alloys [20] ... Generally the obtained coatings were destined to protect the alloys from oxidation and/or corrosion at high temperature. But the technique can also be in some cases used to prevent corrosion at ambient temperature [21].

Concerning specifically the cobalt-based alloys, the surface enrichments in chromium by pack-cementation are also used since several tens of years [22] but they were less studied than the previous ones. The aim of this work is to further explore the possibility of such coating technique for especially the cobalt-based superalloys, by applying cementation process to several model cobalt alloys. Alloys containing a low chromium content (10wt.%Cr) in comparison to what is generally demanded for resistance to high temperature oxidation (about 30wt%) were elaborated for the study. These alloys are either carbide-free (solid solution strengthened alloys) or carbides-containing alloys. Two carbide types out of the most frequently met in cobalt-based superalloys were chosen: chromium carbides on the one hand and tantalum carbides on the other hand. The present study has to define the influence of the alloy's chemical composition and microstructure on the chromium deposition by pack-cementation technique.

2. Experimental procedure

Elaboration of the alloys and metallographic preparation

Several model cobalt-based alloys were initially prepared by foundry practice to allow this study: firstly a simple binary Co-10Cr alloy (named "CoCr"), secondly two Co-10Cr-xC alloys (with x=0.5 wt.% and 1.0 wt.%), and thirdly two quaternary Co-10Cr-xC-yTa alloys (with x=0.25 wt.% and y=4.4wt.%, and x=0.50 wt.% and y=8.7 wt.%) named "CoTa1" and "CoTa2" respectively. These five alloys were synthesized by high frequency induction melting (CELES furnace, 300kHz max.) under inert atmosphere (300mbars of Argon). All initial charges were made of pure elements: Co, Cr, C (graphite) and Ta. The charge (of about 40g) was subjected to a first fusion and the molten alloy was thereafter solidified in the water-cooled copper crucible of the HF furnace. The ingots were then re-melted and the liquid alloys were poured in a cylindrical copper mould to get a cylindrical shape (length 50mm × diameter 10mm). The obtained ingots were cut in order to obtain several disks (diameter 10mm × thickness 2.5mm). One disk per alloy was kept to be mounted in resin and polished with SiC papers from 240-grit to 1200-grit. The final polishing was done using textile paper containing 1µm diamond particles. These samples were metallographically observed to control the initial microstructures using a Scanning Electron Microscope (SEM, type: Philips XL30), mainly in Back Scattered Electrons (BSE) mode and under an acceleration voltage of 20kV.

Pack-cementation runs

The other disks were prepared to be coated and were subjected to cementation. Some of the latter were additionally heat-treated to ensure the inwards diffusion of the deposited chromium. Before cementation, disks were polished up to 1200-grit paper and placed in a silica flask containing the cement. The latter consisted in a mixture of the master alloy (powder of pure Cr), the halide activator (powder of $CrCl_3$) and an inert filler material (powder of Al_2O_3). Secondary vacuum was performed in the silica flask containing the alloy disks and the mixed powders. The flask was closed under vacuum and exposed at 1050°C in a furnace for 7.5h and 15h. After cooling down to ambient temperature, the remaining grains of cement or of alumina were removed from the disk surface by washing under ethanol and by ultrasonically cleaning. For each alloy a 7.5h-cemented disk and a 15h-cemented disk were kept for metallographic characterization while another 7.5h-cemented disk and another 15h-cemented one were isothermally heat-treated at 1200°C for 75h under vacuum, in order to get a deeper chromium enrichment by inwards diffusion of Cr.

Metallographic characterization

The enrichments in chromium on surface and in the sub-surface, just after cementation and after the diffusion heat-treatment, were characterized by concentration profiles measurements using Electron Probe Micro Analysis / Wavelength Dispersion Spectrometry (EPMA-WDS). This was done using Cameca microprobes (SX 50 and SX100), over several hundreds of micrometers in depth and by performing two profiles per sample. X-ray diffraction experiments were also performed in order to determine the nature of the external layer observed at the top of some cemented samples. This was done using a Philips X-pert Pro diffractometer.

3. Results

Initial microstructures.

The chemical compositions (in weight percents) of the alloys are given in Table 1 and the initial microstructures are illustrated by the micrographs presented in Figure 1. The binary alloy seems single-phased while the other alloys are composed of a dendritic matrix and interdendritic carbides. The carbides network is more or less dense depending on the alloy carbon content. Chromium carbides are present in the two Co-10Cr-C alloys while the carbide phase is TaC in the two tantalum-containing alloys. Chromium carbides are logically more present in the Co-10Cr-1.0C alloy than in the Co-10Cr-0.5C one and the tantalum carbides network is significantly more developed in the CoTa2 alloy than in the CoTa1 one.

Sub-surface Cr-enrichment of the Co-10Cr-xC alloys.

After cementation, the mass of the samples has increased for all alloys (Table 2). The mass gain is, as expected, higher for the 15h-cementations (about 16 mg/cm²) than for the 7.5h-cementations (about 12 mg/cm²), but without any evident dependence on the carbon content. The two {chromium carbides} – containing alloys are covered by a continuous layer which appears darker than the substrate when it is observed with the SEM in BSE mode (Figures 2(a) and 2(c) for the Co-10Cr-0.5C, and Figures 3(a) and 3(c) for the Co-10Cr-1.0C). The thickness of this dark layer varies with the carbon content in the alloy and with the cementation duration. Indeed, its thickness increases from 16.5 ±0.6µm to 24.0 ±1.3µm for the Co-10Cr-0.5C alloy and from 20.7 ±2.4µm to 27.2 ±1.9µm for the Co-10Cr-1.0C when the cementation duration increases from 7.5 hours to 15 hours. As revealed by the left parts of the EPMA-WDS profiles presented in Figures 2(b) and 2(d) for the Co-10Cr-0.5C alloy and in Figures 3(b) and 3(d) for the Co-10Cr-1.0C alloy, this dark layer probably consists in a Cr_7C_3 carbide, if the C content, which cannot be directly analyzed by EPMA-WDS, is considered as being the difference to 100% of the sum of the Co and Cr contents. This identification was confirmed by X-Ray Diffraction, as shown by the obtained pattern presented in Figure 4 (Cr7C3 JCPDS 36-1482 [23]). In this pattern one can also notice several peaks of low intensity attributed to the matrix of the cobalt-based alloy.

When a 75h-heat treatment is applied after cementation, the carbide layer disappeared on the surface of the Co-10Cr-0.5C alloy (for the two cementation durations). It still exists on the Co-10Cr-1.0C alloy but it appears thinner than before the heat treatment, since the resulting average thickness decreased to 12.6 ±2.5µm for Co-10Cr-1.0C cemented during 7.5h (Figure 5(a)) and to 17.7 ±0.9µm for Co-10Cr-1.0C cemented during 15h (Figure 5(c)). WDS profiles (Figures 5(b) and 5(d)) show that Cr-diffusion inward the bulk is significantly limited by the presence of this continuous carbide layer on surface. Their left parts also show that the composition of this carbide has changed during the heat-treatment: carbon has obviously diffused from the bulk to penetrate the carbide layer, the type of which has changed for seemingly M_3C_2.

Knowing the carbide type, the chromium mass contained in the carbide layer per surface unit area can be assessed for the samples only cemented, by using the following formula in which m_{Cr}/S is the chromium mass per surface unit area, M_{Cr} and M_C the molar masses of chromium and carbon, ρ_{Cr7C3} the density of the Cr_7C_3 carbide (6.9 g/cm^3) and e_{Cr7C3} the average thickness of the carbide layer: $m_{Cr}/S = [(7\times M_{Cr})/(7\times M_{Cr}+3\times M_C)]\times\rho_{Cr7C3} \times e_{Cr7C3}$. When the results are compared to the mass gains measured after cementation (Table 2), it generally appears that the chromium quantity added to the alloys during cementation is essentially contained in this carbide layer: for example the Cr mass present in the external

carbide layer is equal to 11mg/cm² for the Co-10Cr-0.5C alloy cemented during 7.5h (to compare to12 mg/cm² for the mass gain), and to 18 mg/cm² for Co-10Cr-1.0C cemented for 15h (to compare to 17mg/cm² for the mass gain). The small differences, positive or negative, between the Cr mass in the carbide layer and the mass gain before/after cementation, can be attributed to the fact that the first quantity results from a local measurement while the mass gain difference is a global one (average over the whole sample surface).

Sub-surface Cr-enrichment of the other alloys.

On the contrary, the cementation of the other alloys (CoCr, CoTa1 and CoTa2) led to the incorporation of chromium in their metallic sub-surface without formation of any carbide layer (Figures 6 and 7). Additional grains of chromium cement were still stuck to the surface of the alloys despite washing. As a consequence, a diffusion couple is formed between chromium and the alloys. From several tens of micrometers of depth, depending on the alloy composition and on the cementation time, the chromium content starts increasing from the 10 wt.%Cr in the bulk to reach about 60-65wt.%Cr for the CoCr alloy (formation of a sigma phase between the deposited chromium and the alloy) and about 35wt.% for the CoTa1 and CoTa2 alloys on the extreme surface (Table 3). The chromium quantities added to the samples (Table 2) are here too greater for the 15h-long cementations than for the 7.5h-long cementations. They tend to be also greater for the TaC-containing alloys than for the carbide-free binary CoCr alloy, and for all the latter greater than for the two Co-10Cr-xC alloys.

The 75h-heat treatment induced the disappearance of the Cr cement grains initially stuck on surface. In the same time chromium, present in the cement grain or already incorporated in the sub-surface, diffused deeper in the alloys (Figures 8 and 9, Table 4). This resulted in a decrease in maximal Cr content of the external surface (Table 3). The latter fell from more than 60 wt.% down to 33-34 wt.% Cr in the case of the CoCr alloy, with consequently the disappearance of the sigma phase. The decrease is more limited for the CoTa1 and CoTa2 alloys since the maximal Cr content on extreme surface is slightly lower than 30wt.%. After heat treatment the external zone of alloy enriched in chromium (Table 4) is thicker for the two tantalum-containing alloys (220-230µm for CoTa2 and 190-200µm for CoTa1) than for the binary CoCr (150-160µm), and for the TaC-richest CoTa2 than for CoTa1. Concerning the sample masses, they remained obviously the same as before heat treatment.

4. Discussion

The pack-cementation runs performed for the different cobalt-based alloys resulted in a significant sub-surface enrichment in chromium in all cases. However two different results are obtained in term of surface coatings, depending on the chemical composition and/or the microstructure of the alloy.

The chromium deposit on the Co-10Cr, CoTa1 and CoTa2 substrates results in the formation of a metallic outer part enriched in chromium. In these cases, the cementation processes led to a significant enrichment in chromium (more than 33wt.%Cr and even up to 60-65wt.%Cr for the binary alloy) in the most external part of the alloy. It should be noted that the chromium grains did not result from the cementation process itself but of the sintering of the cement on the surface of alloys during the process. If required, such grains can be avoided by isolating the cement from the alloy (in the present study, the presence of some chromium grains at the surface of the samples after cementation was not a problem since heat treatment was performed after cementation).

For the binary Co-10Cr, an intermediate layer of sigma phase formed between the Cr layer and the alloy during the process. The Cr content in the cobalt matrix rose 30% at the sigma/Co matrix interface. These data are in good agreement with the Co-Cr phases diagram at 1050°C. In the case of the Ta-containing alloys, the sigma phase was not observed. The cobalt matrix, containing chromium, is then directly in equilibrium with the stick chromium grains after the cementation runs.

Fortunately the sigma brittle phase disappeared during the diffusion heat-treatment because of the inward penetration of chromium resulting in a general lowering of the chromium content and a deeper distribution. The maximal concentration in chromium in the external zone of the Co-10Cr alloy rose 32-35wt.%Cr after the heat treatment. In the part of the alloy concerned with chromium diffusion, the Cr-concentration evolves in depth according to the typical profile expected in the case of diffusion in solid state in single phase.

With the CoTa1 and CoTa2 alloys, the Cr-concentration profiles after heat treatment are somewhat the same as in the binary alloys. However, the maximal chromium concentration did not exceed 30wt.%. The inward diffusion of chromium was significantly higher in the case of the CoTa1 and CoTa2 alloys than in the binary one. This can be the result either of the preferential diffusion along interfaces existing between the matrix and the carbide network, or of a slower diffusion in sigma phase than in the cobalt matrix in the case of Co-10Cr. Hence, the chromium content in the most external zone of the alloys remains after heat treatment at a level significantly higher than the initial chromium content in the bulk (at least 30wt.% against 10wt.% in the bulk) for the three considered alloys,

A second type of behavior observed during cementation was displayed by the two Co-10Cr-xC alloys. The cementation process is, in this case, not only controlled by Cr diffusion in the metallic sub-surface of the alloys but mainly by the interdiffusion of chromium and carbon. This results in the formation, in the external part, of a continuous and compact carbide layer which hindered the chromium inward diffusion. This phenomenon was already encountered after Cr-coatings by pack-cementation on various materials containing carbon: metallic alloys (e.g. carbon steels [24,25]) or ceramic materials (SiC [26]). Such carbide layer can be desired, for example to achieve high surface hardness and wear resistance [27], but also it can be absolutely unwanted because it can exhibit brittle behavior. Its appearance can be avoided by optimizing the treatment conditions [28]. Such chromium carbide layer can eventually play a protective role against high temperature oxidation but its easy spallation [29] when temperature varies can have catastrophic consequences. Such spallation is what probably appended in the present work for the Co-10Cr-0.5C sample which had obviously lost its carbides layer, as observed when it was examined after the 75h-heat treatment. Another possible drawback associated to the development of such carbide layer is that the heat treatment performed at 1200°C obviously led to the diffusion, not only of chromium inward the bulk, but also of carbon in the opposite direction leading to the dissolution of the nearest chromium carbides. The former consequence is the change of the stoechiometry of the carbide layer to a richer one ($Cr_7C_3 \rightarrow Cr_3C_2$) and the second one is the disappearance of the outer bulk's chromium carbides during the heat treatment, clearly visible in the SEM micrographs of Figures 5(a) and 5 (c) by comparison to Figures 3(a) and 3(c). Then the mechanical properties of this part of the bulk can be weakened.

The deposit of chromium by pack-cementation on the studied carbides-containing cobalt alloys is strongly influenced by the nature of the carbide type, i.e. chromium carbides or tantalum carbides. The differences observed have to be explained regarding the stability of these carbides at high temperature. In the first case the existence of a very high activity in chromium on surface destabilized the existing chromium carbides of the nearest part of the bulk. It also induced the diffusion of carbon atoms outward, with as consequence the growth and the thickening of the external carbide layer. Thus the chromium carbides initially present

in the alloy disappear, or at least become less present, over an increasing depth. Such an impoverishment of the alloys in chromium carbides was effectively observed. On the contrary, if the carbides initially present in the bulk are more stable at high temperature, as the TaC carbides of the CoTa1 and CoTa2 alloys, the high chromium activity on extreme surface cannot induce a destabilization of these carbides and practically no carbon is available to diffuse outward. Then no carbide layer formed on surface.

Most of the commercial cobalt-based alloys necessarily need to be mechanically reinforced by primary interdendritic carbides, as well as by secondary fine carbides precipitated in matrix to combat dislocation's movement under stress. Then several types of carbides can be initially present in such alloys: chromium carbides (e.g. Cr_7C_3), MC carbides (e.g. TaC), … If the sub-surface Cr-enrichment by pack-cementation must be realized without appearance of an external carbide layer, chromium carbides must be avoided: primary and secondary Cr_7C_3 carbides (as shown here), but also probably $Cr_{23}C_6$. On the contrary no such restriction concerns the presence of tantalum carbides in the bulk since they did not promote the appearance and the growth of such an external carbide layer.

5. Conclusions

Sub-surface-enrichment in chromium of 10wt.%Cr-containing cobalt-based alloys by pack-cementation is possible and can lead to an outer zone containing more than 30wt.%.Cr. However the presence of carbon in the alloys may promote the formation of a carbide layer which localized chromium in the external part of the piece. The layer may leave the substrate during thermal cycling and then expose the latter to catastrophic oxidation. To avoid such phenomenon the carbides strengthening the alloy must be more stable than the chromium carbides. Then no external carbide layer forms during cementation, as demonstrated in the case of the alloys containing exclusively TaC carbides which are often used in cobalt-based superalloys if creep-resistance at very high temperature is required. If the alloy does not contain carbides or if these ones are stable, the results presented in this work for a binary Co-10Cr alloy and for two alloys containing exclusively TaC, showed that a cementation run for several hours at 1050°C, followed by a heat treatment at 1200°C for several tens of hours, lead to the required sub-surface enrichment in chromium (near 30wt.%Cr). The effect of this coating on the oxidation resistance will be studied at high temperature in the second part of this work [30].

Acknowledgments

The authors wish to thank Guillaume Aubert for its technical help, and the Common Service of Microscopy and Microanalysis of the University Henri Poincaré Nancy 1, notably Sullivan De Sousa for the microprobe analyses.

References

[1] C.T. Sims, W.C. Hagel, The Superalloys, John Wiley&Sons, New York, 1972.
[2] D.J. Young, High Temperature Oxidation and Corrosion of Metals, Elsevier, Amsterdam, 2008.

[3] A.M. Beltram, Cobalt-base alloys, in C.T. Sims, N.S. Stoloff, W.C. Hagel, Superalloy II – High Temperature Materials for Aerospace and Industrial Power, John Wiley-Interscience, New York, 1987, 135-163.
[4] B.A. Pint, P.F. Tortorelli, I.G. Wright, Oxid. Met. 58 (1/2) (2002) 73-101.
[5] F. Zamoum, T. Benlaharche, N. David, R. Podor, M. Vilasi, Intermetallics, 16(4) (2008) 498-507.
[6] G. Slama, A. Vignes, Journal of Less Common Metals, 23(4) (1971) 375-393.
[7] M.J. Fleetwood, Journal of the Institute of Metals, 98 (1970) 1-7.
[8] S.R. Levine, R.M. Caves, Journal of the Electrochemical Society, 121(8) (1974) 1051-1064.
[9] M.R. Jackson, J.R. Rairden, Journal of Vacuum Science & Technology, 17(1) (1980) 77-80.
[10] A.N. Mukherji, P. Prabhakaram, Anti-Corrosion Methods and Materials, 25(1) (1978) 4-8.
[11] K. Schneider, R. Bauer, H.W. Grünling, Thin Solid Films, 54(3) (1978) 353-357.
[12] S.C. Singhal, Thin Solid Films, 45(2) (1977) 321-329.
[13] S.C. Singhal, Thin Solid Films 53(3) (1978) 375-381.
[14] M. Kornmann, J. Rexer, P. Dancoisne, E. Anderson, Metals Technology 4(4) (1977) 218-222.
[15] M. Bateni Reza, S. Shaw, P. Wei, A. Petric, Materials and Manufacturing Processes, 24(6) (2009) 626-632.
[16] C. Choux, S. Chevalier, Y. Cadoret, Materials Science Forum, 595-598 (2008) 41-49.
[17] F. Rioult, N. Sekido , R. Sakidja, J.H. Perepezko, Journal of the Electrochemical Society, 154(11) (2007) C692-C701.
[18] M. Vilasi, J. Steinmetz, B. Gaillard-Allemand, B. Berton, P. Chéreau, Journal of Advanced Materials, 32(2) (2000) 53-57.
[19] X.P. Guo, L.X. Zhao, P. Guan, K. Kusabiraki, Materials Science Forum, 561-565 (2007) 371-374.
[20] S. Majumdar, I.G. Sharma, A.K. Suri, International Journal of Refractory Metals and Hard Materials, 26(6) (2008) 549-554.
[21] J.S. Park, J.M. Kim, H.Y. Kim, C.S. Kang, S.W. Choi, Materials Science Forum, 638-642 (2010) 793-798.
[22] G.H. Faber, Proceeding of the conference High Temperature Alloys for Gas Turbines, Liege (Belgium) 25th – 27th September 1978.
[23] X-ray powder diffraction database: Joint Committee on Powder Diffraction Standards/the International Center for Diffraction Data (JCPDS/ICDD), 1999 PCPDFWIN Version 2.02.
[24] V.R. Behrani, P.M. Singh, Proceeding of the conference Corrosion 2007, Nashville (USA) 11th to 15th March 2007.
[25] J.W. Lee, J.G. Duh, Proceeding of the conference Multiphase Phenomena and CFD Modeling and Simulation Materials Processes, Charlotte (USA) 14th to 18th March 2004.
[26] S.C. Kung, Oxidation of Metals 42 (3-4) (1994) 191-203.
[27] J.W. Lee, J.G. Duh, S.Y. Tsai, Surface and Coatings Technology (153) (2002) 59-66.
[28] M. Zheng, R.A. Rapp, Oxidation of Metals 49(1-2) (1998) 19-31.
[29] X.Peng, J.Yan, C.Xu, F.Wang, Metallurgical and Materials Transactions A, 39A, 119-129.
[30] G. Michel, P. Berthod, M. Vilasi, S. Mathieu, P. Steinmetz, Surface and Coatings Technology, submitted.

Table 1 The targeted and obtained compositions (in wt.%) of the alloys (average value ± standard deviation resulting from three EPMA-WDS measurements in not-focalized mode at ×400)

alloys conditions	**Cr**		**Ta**	
	Targeted	obtained	**Targeted**	obtained
CoCr	**10.0**	10.4 (±0.1)	**/**	/
Co-10Cr-0.5C	**10.0**	10.0 (±0.1)	**/**	/
Co-10Cr-1.0C	**10.0**	10.0 (±0.1)	**/**	/
CoTa1 (0.25C)	**10.0**	10.3 (±0.1)	**4.35**	4.5 (±0.4)
CoTa2 (0.50C)	**10.0**	10.5 (±0.1)	**8.70**	8.5 (±1.5)

Table 2 Average mass gain (mg/cm²) observed for the two times of cementation (average values calculated for four cemented samples (difference of the sample masses measured after and before)

alloys cementation duration	CoCr	Co-10Cr-0.5C	Co-10Cr-1.0C	CoTa1	CoTa2
7.5h	16	12	11	23	21
15h	**25**	**16**	**17**	**32**	**24**

Table 3 Chromium contents (wt.%) on the external surface of the {carbide layer}–free alloys after cementation and/or diffusion heat-treatment (average value ± standard deviation) from two EPMA-WDS profiles

alloys conditions	**CoCr**	**CoTa1**	**CoTa2**
C7.5h only	**65.0** ±2.6	**34.1** ±4.7	**36.2** ±1.4
C15h only	**61.3** ±1.6	**33.0** ±1.7	**34.5** ±3.1
C7.5h HT75h	**33.2** ±0.5	**29.3** ±0.5	**29.1** ±0.5
C15h HT75h	**34.2** ±1.4	**29.3** ±0.3	**29.4** ±0.6

Table 4 Depths (µm) enriched in chromium resulting from cementation and/or diffusion heat-treatment for the {carbide layer}–free alloys (average value ± standard deviation), from two EPMA-WDS profiles

alloys conditions	**CoCr**	**CoTa1**	**CoTa2**
C7.5h only	**38** ±14	**26** ±2	**20** ±6
C15h only	**58** ±14	**42** ±6	**41** ±5
C7.5h HT75h	**154** ±6	**190** ±6	**224** ±21
C15h HT75h	**156** ±3	**196** ±2	**231** ±13

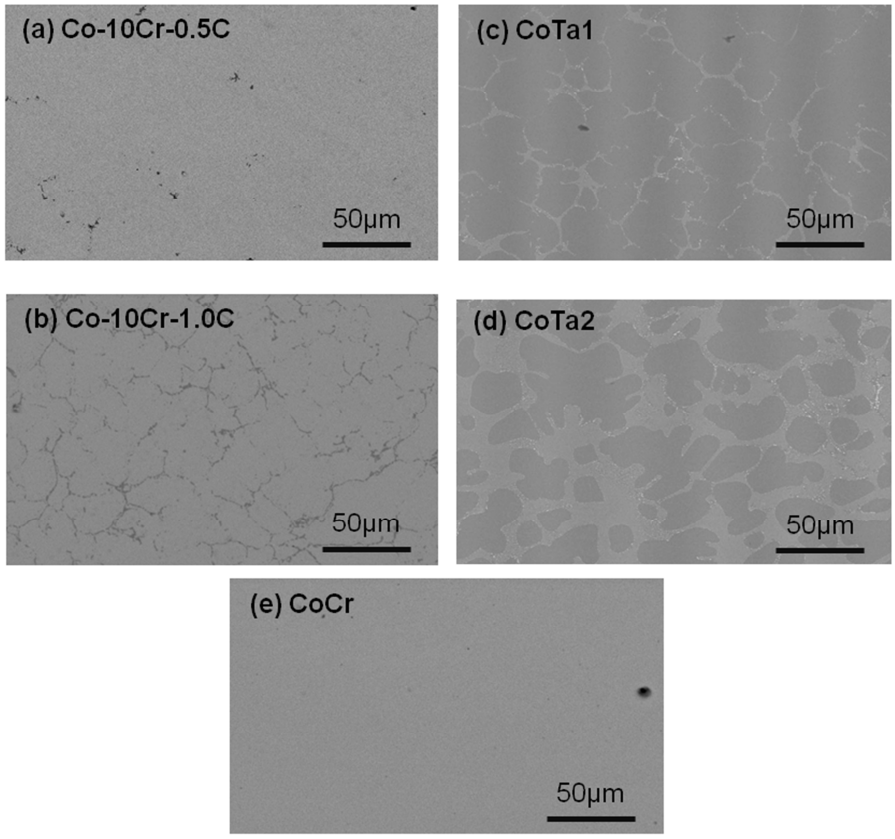

Figure 1 Microstructures of the initial alloys (SEM micrographs, taken in BSE mode)

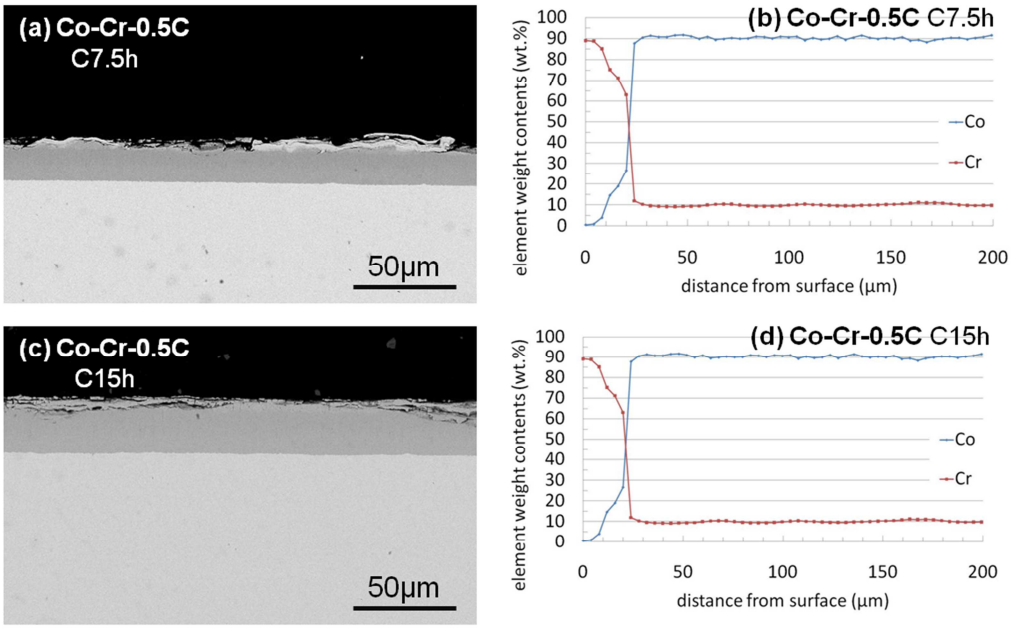

Figure 2 SEM micrographs of the external Cr_7C_3-layer formed on the Co-10Cr-0.5C alloy after 7.5h (a) and 15h (c) of cementation; EPMA-WDS profiles performed perpendicularly to surface from the carbide layer revealing the very low Cr-enrichment of the alloy under the carbide layer after 7.5h (b) and 15h (b) of cementation

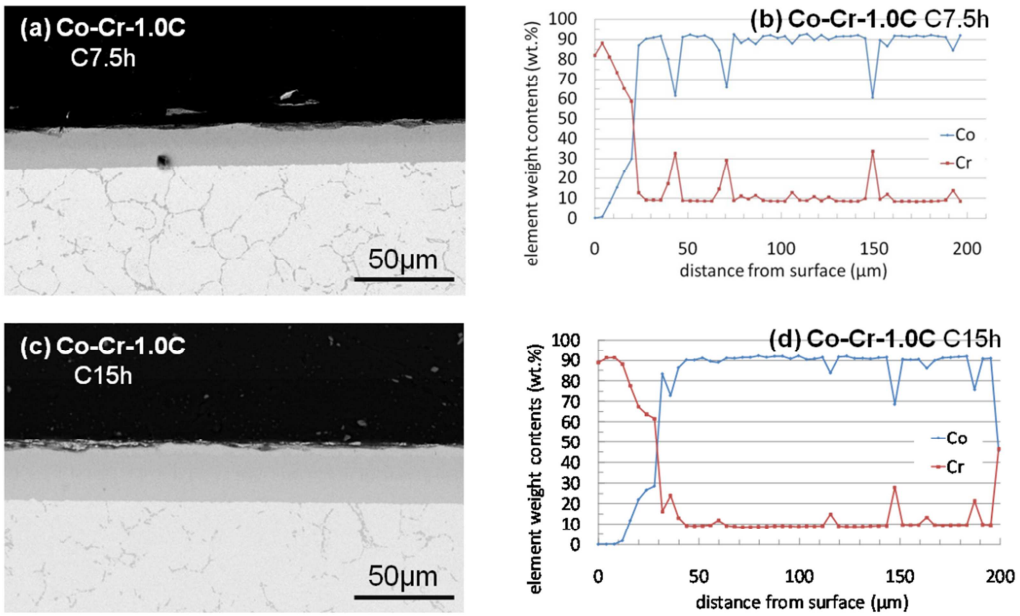

Figure 3 SEM micrographs of the external Cr_7C_3-layer formed on the Co-10Cr-1.0C alloy after 7.5h (a) and 15h (c) of cementation; EPMA-WDS profiles performed perpendicularly to surface from the carbide layer revealing the very low Cr-enrichment of the alloy under the carbide layer after 7.5h (b) and 15h (b) of cementation

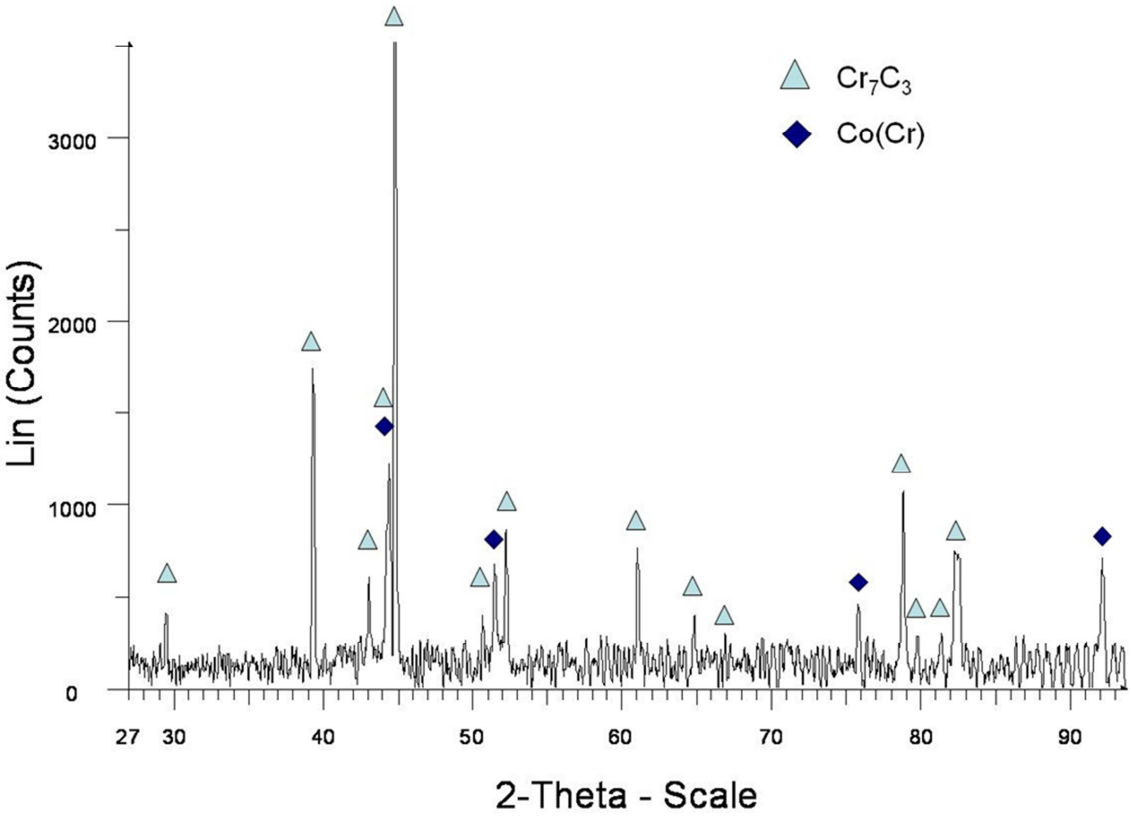

Figure 4 Example of XRD pattern obtained on the surface of a cemented Cr-10C-xC alloy; confirmation that the external carbide layer formed during cementation is Cr_7C_3

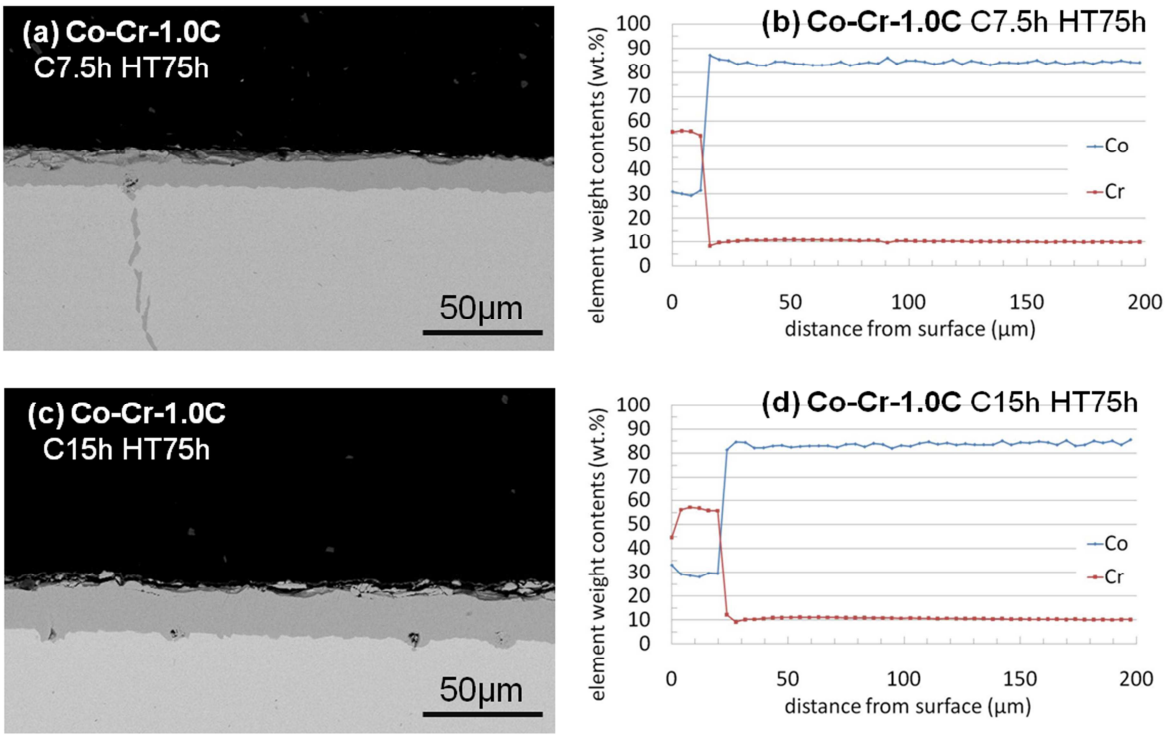

Figure 5 SEM micrographs of the Co-10Cr-1.0C alloy heat-treated during 75h at 1200°C after 7.5h-long or 15h-long cementation); EPMA-WDS profiles performed perpendicularly to surface from the carbide layer revealing the very low Cr-enrichment of the alloy under the carbide layer ((b) and (d)) and the composition change of the latter (about 40 at.%Cr – 20 at.%Co – 40 at.%C, i.e. M_3C_2)

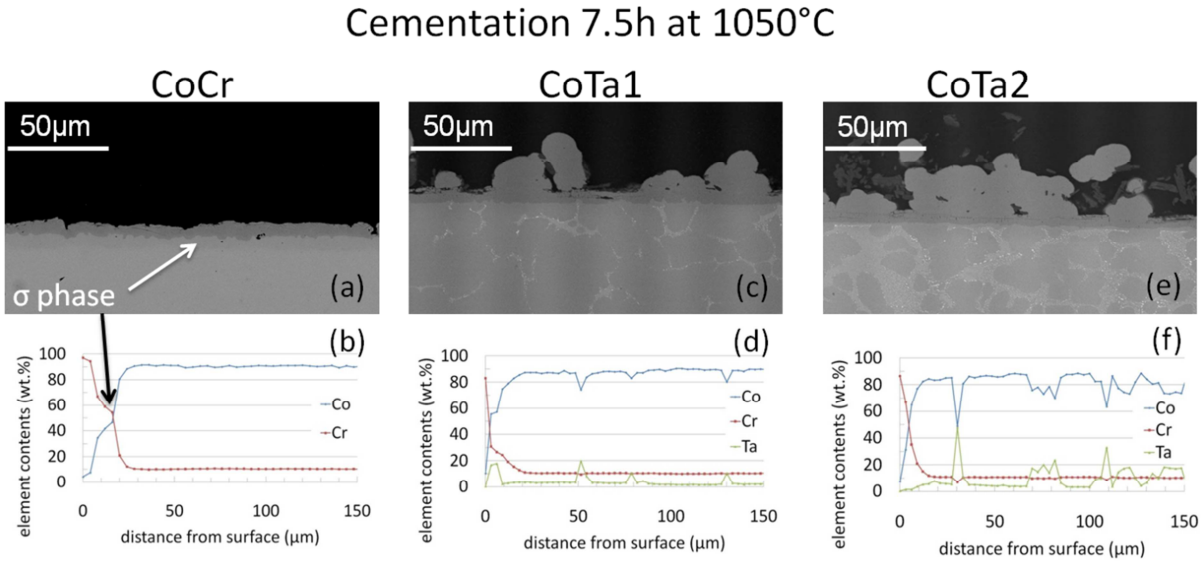

Figure 6 Sub-surface states after cementation for 7.5h at 1050°C: SEM micrographs of the CoCr alloy's surface (a), of the CoTa1 alloy's surface (c) and of the CoTa2 alloy's surface (e); sub-surface enrichments in chromium of the binary CoCr alloy (b), of the CoTa1 alloy (d) and of the CoTa2 alloy (f)

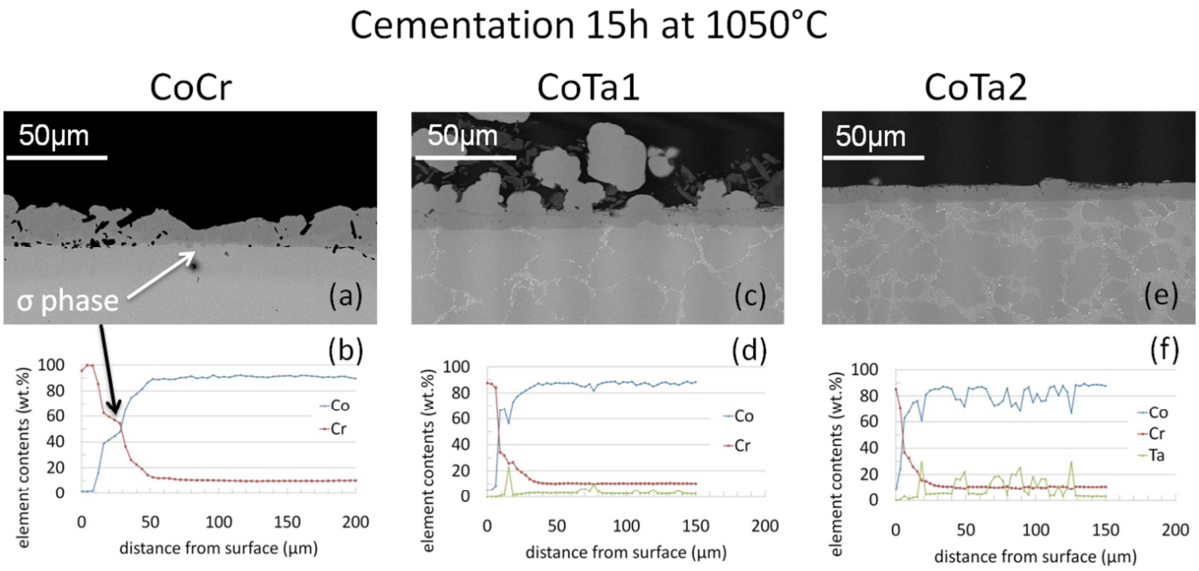

Figure 7 Sub-surface states after cementation for 15h at 1050°C: SEM micrographs of the CoCr alloy's surface (a), of the CoTa1 alloy's surface (c) and of the CoTa2 alloy's surface (e); sub-surface enrichments in chromium of the binary CoCr alloy (b), of the CoTa1 alloy (d) and of the CoTa2 alloy (f)

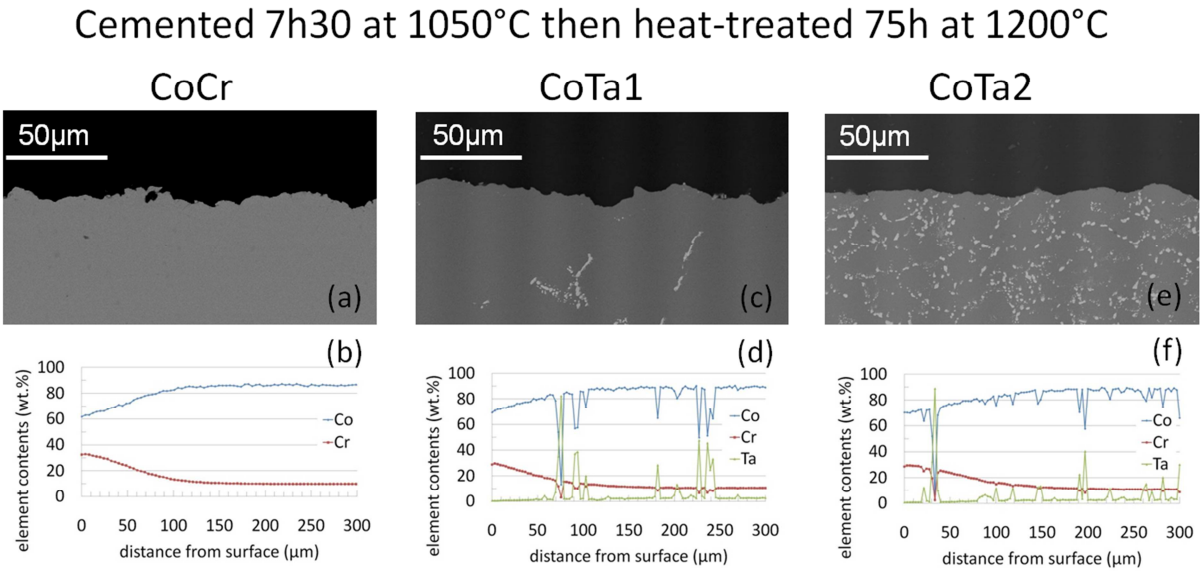

Figure 8 Sub-surface states after cementation for 7.5h at 1050°C and heat-treatment at 1200°C for 75h: SEM micrographs of the CoCr alloy's surface (a), of the CoTa1 alloy's surface (c) and of the CoTa2 alloy's surface (e); sub-surface enrichments in chromium of the binary CoCr alloy (b), of the CoTa1 alloy (d) and of the CoTa2 alloy (f)

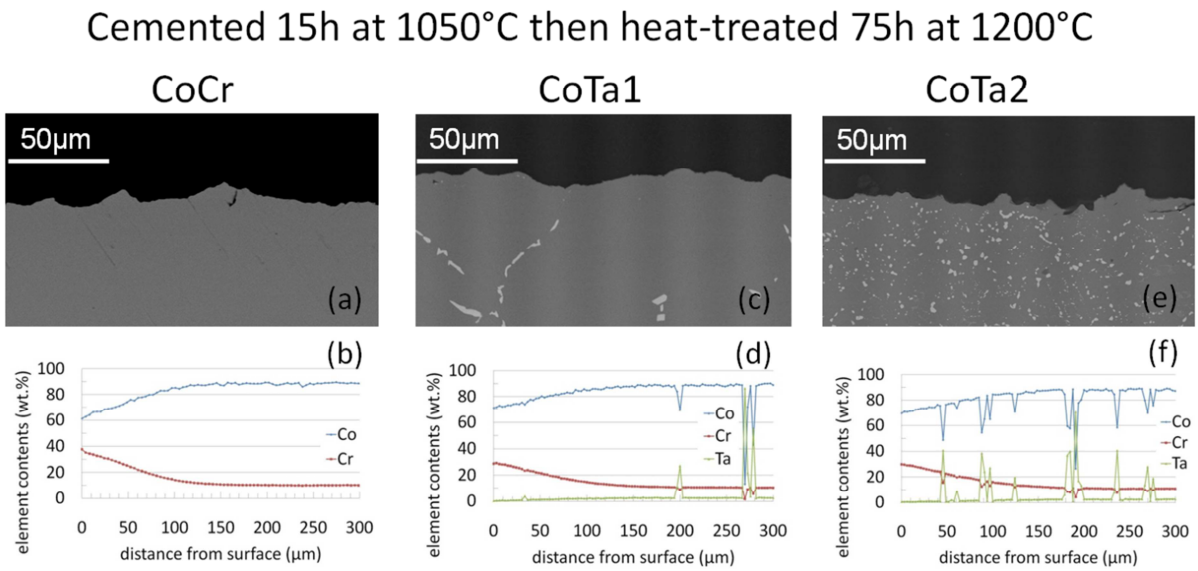

Figure 9 Sub-surface states after cementation for 15h at 1050°C and heat-treatment at 1200°C for 75h: SEM micrographs of the CoCr alloy's surface (a), of the CoTa1 alloy's surface (c) and of the CoTa2 alloy's surface (e); sub-surface enrichments in chromium of the binary CoCr alloy (b), of the CoTa1 alloy (d) and of the CoTa2 alloy (f)